ATMOSPHERIC SCIENCE LETTERS
*Atmos. Sci. Let.* **18**: 484–490 (2017)
Published online 23 November 2017 in Wiley Online Library
(wileyonlinelibrary.com) **DOI:** 10.1002/asl.792

RMetS
Royal Meteorological Society

# Analysis of euphotic depth in snow with SNICAR transfer scheme

Efang Zhong,[1,2] Qian Li,[1]* Shufen Sun,[1] Shangfeng Chen[1] and Wen Chen[1]

[1]*Center for Monsoon System Research, Institute of Atmospheric Physics, Chinese Academy of Sciences, Beijing, China*
[2]*College of Earth Sciences, University of Chinese Academy of Sciences, Beijing, China*

*Correspondence to:
*Q. Li, Center for Monsoon System Research, Institute of Atmospheric Physics, Chinese Academy of Sciences, #40 Huayanli, Qjjiahuozi, Chaoyang District, Beijing, 100029, China.*
*E-mail: qian@mail.iap.ac.cn*

Received: 6 June 2017
Revised: 6 October 2017
Accepted: 11 October 2017

## Abstract

**Solar radiation in the visible spectrum can penetrate through snowpack to a considerable depth, which is named as the euphotic depth in snow. If the snow depth is no greater than the euphotic depth, the surface albedo is greatly affected by the underlying surface. This study defines the euphotic depth as the depth where the residual solar radiation in snow began to be less than 1.0 W $m^{-2}$ and provides a convenient approach to estimate it. A two-stream, multilayer radiation penetration model (SNow, ICe, and Aerosol Radiation) was applied to predict the vertical profiles of solar radiation based on regular measurements of snow pits and downward solar radiation at Col de Porte (CDP), France from 1993 to 2011. The euphotic depth in snow at CDP exhibits clear seasonal variations, with median values in winter months of 6.8, 8.8, and 10.5 cm, and those in spring remaining nearly on the same level (24.4 and 24.2 cm). The maximum euphotic depth at CDP reached as deep as 78 cm. Further analyses demonstrated that the euphotic depth in snow is related to not only the external initial solar irradiance but also the interior snow extinction coefficient. Stronger illumination and smaller snow extinction coefficients may correspond to greater euphotic depths in snowpack.**

**Keywords:** **euphotic depth; SNICAR; incident radiation; extinction coefficient**

## 1. Introduction

Snow is translucent such that solar radiation in the visible spectrum can penetrate through the snowpack to a considerable depth (e.g. Giddings and Lachapelle, 1961; Baker *et al.,* 1991; Flanner and Zender, 2005). The underlying surface has a great influence on surface albedo if the incident solar radiation can penetrate to the bottom of the snowpack (e.g. O'Neill and Gray, 1972). Wiscombe and Warren (1980) indicated that the surface albedo of a shallow snowpack is substantially different from that of deep snowpack, especially in the visible spectrum. Hence, special attention should be given to shallow snowpack cases in snow albedo and snow model studies. However, how to distinguish shallow snowpack from deep snowpack has been controversial.

Many general circulation models (GCMs) parameterize grid-average albedos ($\alpha$) as weighting functions ($f_s(h_s)$) of snow depth ($h_s$) (e.g. Hansen *et al.,* 1983; Verseghy, 1991; Dickinson *et al.,* 1993; Douville *et al.,* 1995; Cox *et al.,* 1999),

$$\alpha = f_s\left(h_s\right)\alpha_s + \left(1 - f_s\left(h_s\right)\right)\alpha_0, \qquad (1)$$

where $\alpha_s$ is the albedo of deep, homogeneous snow, and $\alpha_0$ is the albedo of the snow-free surface. Equation (1) illustrates that albedo increases with the enhancement of snow depth in shallow snowpack, and that albedo tends to be independent of the underlying surface after the snowpack reaches a certain depth ($h_0$, the threshold of deep snowpack). Various empirical expressions for $f_s(h_s)$ in different GCMs contribute to various thresholds (Armstrong and Brun, 2008, figure 4.13). Gray and Landine (1987) set 25 cm as a reference depth to discriminate between deep or shallow snow cover for the respective snow albedo decay rates. Baker *et al.* (1991) indicated that 5, 7.5, and 15 cm of snow over bare soil, sod, and alfalfa, respectively, is required to mask the underlying surface effectively. That is to say, there is no fixed standard to differentiate clearly between deep and shallow snowpack. In principle, the key is to compare the snow depth ($h_s$) with the euphotic depth ($z_{eu}$), which is the path depth to which incident solar radiation is transmitted in the snowpack. If $h_s > z_{eu}$, then the snowpack is classified as deep snowpack. $h_s$ is easily measured, and $z_{eu}$ can be calculated with knowledge of light transmission in the snowpack.

Bohren and Barkstrom (1974) stated that incident solar radiation attenuates exponentially with increasing depth in the snowpack. The transmission can be expressed as follows:

$$F_{\downarrow}(z + \Delta z, \lambda) = F_{\downarrow}(z, \lambda)\exp\left(-k_{\lambda}\Delta z\right), \qquad (2)$$

where $k_{\lambda}$ represents the 'asymptotic flux-extinction coefficient' at a particular wavelength $\lambda$, and $F_{\downarrow}(z, \lambda)$ denotes the spectrum solar radiation at level $z$ (Brandt and Warren, 1993).

Several studies have investigated the solar radiation transmission in snowpack. Järvinen and Leppäranta (2013) measured the solar radiation above and inside the snowpack, and found that the mean spectral

diffuse extinction coefficient varied between 0.04 and 0.31 $cm^{-1}$ (10–20 cm layer). They further inferred that the euphotic depth ($z_{eu}$) was approximately 50 cm at which the broadband irradiance was 1% of the downward irradiance at the surface. Baker *et al.* (1991) indicated that the extinction coefficient ranges from 0.07 to 1.5 $cm^{-1}$.

These investigations were based on direct measurements of solar radiation profiles. However, solar radiation transmission measurements through snow are notoriously difficult, since light levels beneath the snow are quite weak. Furthermore, spectral dependence complicates the measurements, not to mention the problem of inserting the sensor without disturbing the snowpack (Perovich, 2007). Model simulations represent an alternative approach and can provide a preliminary estimation of the light transmission profile.

In light of the above, this study aimed to investigate the euphotic depth in snowpack and to answer the question as to how thick a snowpack should be before it can be regarded as a deep or shallow snowpack. Specifically, a method of detecting the euphotic depth is proposed. The method applies a two-stream, multilayer radiation penetration model [SNow, ICe, and Aerosol Radiation (SNICAR)] to estimate the vertical distribution of solar radiation based only on regular measurements of snow pits and the initial downward solar radiation. Furthermore, seasonal variability in the euphotic depth and possible key factors are discussed.

## 2. Methods and data

### 2.1. Definition of the euphotic depth in snow

This study defines the euphotic depth in snow as the depth at which the residual solar radiation begins to be $<1.0\ W\ m^{-2}$. If the residual solar radiation at the bottom of the snowpack is $\geq 1.0\ W\ m^{-2}$, which means the light has penetrated through the snowpack completely, then it is a shallow snowpack. In this case, the euphotic depth is equal to the snow depth. Reason for this definition is given in Section 3.3 with detailed examples.

### 2.2. SNow, ICe, and Aerosol Radiation

The vertical profiles of solar radiation in snowpack are predicted by the SNICAR model (Flanner and Zender, 2005, 2006), which employs the theory proposed by Wiscombe and Warren (1980) and a two-stream radiative transfer solution from Toon *et al.* (1989). Because the attenuation of solar radiation in snow varies strongly across the solar spectrum, the solar fluxes are computed in five spectral bands: one in the visible (0.3–0.7 $\mu$m) and four in the near-infrared spectra (i.e. 0.7–1.0, 1.0–1.2, 1.2–1.5, and 1.5–5.0 $\mu$m, respectively). In SNICAR, snow is considered to be made up of a collection of ice spheres, with a lognormal distribution of the optical effective radius over 50–1500 $\mu$m. Ice Mie scattering parameters, which depend on grain radius and spectral bands, are derived offline for computational efficiency (Oleson *et al.,* 2010). A number of validations and evaluations of SNICAR have been conducted and have demonstrated that SNICAR is solid and robust in calculating snow albedo and radiation transmission (e.g. Hadley and Kirchstetter, 2012; Meinander *et al.*, 2013; Zhong *et al.,* 2017). In addition, SNICAR has been incorporated into the Community Land Model (CLM) version 4 (Oleson *et al.,* 2010).

The required input variables mainly include: incident radiation, solar zenith angle, snowpack depth and density, and snow grain optical effective radius. Most of these variables can be obtained from measurements directly, as described in Section 2.3. The snow grain optical effective radius can be calculated from the snow specific surface area (SSA), as described in Section 2.4.

### 2.3. Data from Col de Porte, France

The data used in this study are derived from the snow and meteorological research station Col de Porte (CDP), France (43.3°N, 5.77°E, ~1325 m altitude). This site has been used for over 50 years for development and evaluation of snow models (e.g. Brun *et al.,* 1989; Chen *et al.,* 2014). The measurements in this study were collected in 1993–2011, including the following: (1) manual snow pit observations containing vertical profiles of snow density and snow grain type. Each snow pit (a total of 302 pits) observation was carried out approximately weekly throughout the duration time of snow cover, covering snow accumulation, and melting season; (2) corresponding surface incident direct and diffuse shortwave radiation.

More details can be found in Morin *et al.* (2012) and are available on the following website: http://epic.awi.de/30060/. Figures 1(a) and (b) show an example of the profiles of snow density and snow grain type, respectively, at CDP in winter 2010.

### 2.4. Optical effective radius

The other required inputs for SNICAR are the snow grain optical effective radius ($r_{opt}$). This variable is the surface area-weighted mean radius of an ensemble of ice spheres and is directly related to the SSA (Flanner and Zender, 2006), as follows:

$$r_{opt} = \frac{3.0}{\rho_{ice} \times SSA}, \tag{3}$$

where $\rho_{ice}$ denotes the density of ice (917 $kg\ m^{-3}$).

Domine *et al.* (2008) proposed a parameterization scheme of the snow SSA from an examination of snow crystal types and a measurement of snow density. Morin *et al.* (2013) verified this parameterization scheme and found that it performed rather satisfactorily, both qualitatively and quantitatively. Hence, following the scheme proposed by Domine *et al.* (2008), this study estimated the value of the snow SSA from snow type and snow density, which are included in the snow stratigraphy

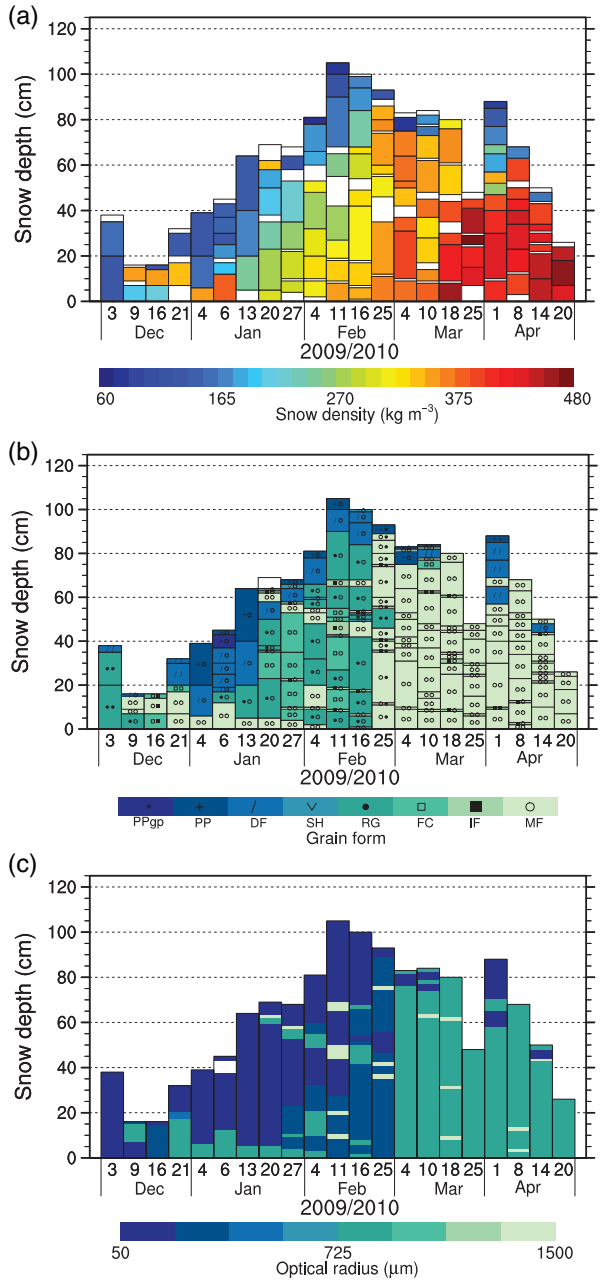


**Figure 1.** Example of profiles at CDP in winter 2010. (a) Measurements of snow density; (b) measurements of snow type; and (c) simulations of snow optical radius from snow density and snow type. Text descriptions of the snow type abbreviations are listed in Table 1. Box in white indicates missing data.

measurements in Section 2.2. Details of the snow SSA parameterization scheme are listed in Table 1. Then, the effective optical radius can be calculated by Equation (3).

In this way, Figure 1(c) shows the corresponding snow grain effective radius. Vertically, snow at upper layers tends to have a lower density and smaller effective grain radius than that at lower layers. Snow compaction accounts for these phenomena. Horizontally, younger snow shows the similar characteristics, by contrast with the older snow. Snow metamorphism contributes to the differences between young and old snow.

### 2.5. Extinction coefficient

In solar radiation observations, the transmission of the incident radiation can be simplified as follows (Brandt and Warren, 1993):

$$F_{\downarrow}(h) = F_{\downarrow}(0)\exp\left(-\int_0^h \bar{k}(z)\,dz\right), \qquad (4)$$

where $F_{\downarrow}(h)$ denotes the net solar radiation at depth of $h$, $F_{\downarrow}(0)$ represents the net solar radiation at the surface, and $\bar{k}(z) = -(1/\Delta z)\ln\left(\frac{\int F_{\lambda,\downarrow}(0)\exp[-k_\lambda(z+\Delta z)]d\lambda}{\int F_{\lambda,\downarrow}(0)\exp(-k_\lambda z)d\lambda}\right)$, it denotes the 'local bulk-extinction coefficient' for the total solar radiation at level $z$ in the snowpack.

To concisely reflect the snow optical properties of a whole snow layer, a mean extinction coefficient ($\tilde{k}$) of the whole snow layer (from the surface to depth $h$) is better than a local extinction coefficient ($\bar{k}(z)$). The mean extinction coefficient ($\tilde{k}$) is defined as follows:

$$\exp\left(-\int_0^h \bar{k}(z)\,dz\right) = \exp\left(-\tilde{k}\Big|_h h\right),$$

$$\tilde{k}\Big|_h = \frac{\int_0^h \bar{k}(z)\,dz}{h}. \qquad (5)$$

Combining Equation (4) with Equation (5), it can be expressed as,

$$\tilde{k}\Big|_h = \frac{\int_0^h \bar{k}(z)\,dz}{h} = -(1/h)\ln\left(\frac{F_{\downarrow}(h)}{F_{\downarrow}(0)}\right). \qquad (6)$$

## 3. Results

### 3.1. Euphotic depth at CDP and its seasonal variability

Euphotic depths in the snowpack at CDP in 1993–2011 were estimated as described in Section 2.1. In addition, the required vertical distributions of solar radiation are predicted by SNICAR, using the incident radiation, solar zenith angle, snow depth and density, and optical effective radius as inputs.

Figure 2(a) presents the euphotic depth of 302 snow pits at CDP in 1993–2011. The red points (25 in total) mean that the light has already penetrated through the snowpack, while the blue points (277 in total) are the normal cases. The euphotic depths at CDP exhibit a concentrated distribution in winter days, but show a more varying distribution in spring days.

Figure 2(b) presents a boxplot for the euphotic depth grouped by month. The ranges of distributions of monthly $z_{eu}$ become wider gradually, and the extremes become greater. The monthly maximum values of $z_{eu}$ in December, January, February, March, and April are 32.4, 46.0, 57.0, 67.0, and 78.0 cm, respectively. Baker *et al.* (1991) indicated that shortwave radiation can penetrate to a depth of 100 cm. The monthly median values of $z_{eu}$ in winter months (December, January, and February) are very close to each other (6.8, 8.8, and 10.5 cm,

**Table 1.** Snow SSA parameterizations based on snow type and snow density, following Domine *et al.* (2007) and Morin *et al.* (2013).

| No | Snowtype | Text description | SSA ($m^2\ kg^{-1}$) from snow type and density ($kg\ m^{-3}$) |
|---|---|---|---|
| 1 | PP | Precipitation particles | $SSA = -17.41 \ln(\rho) + 150.90$ |
| 2 | PP (DF) | Precipitation particles/decomposing fragments | $SSA = -16.05 \ln(\rho) + 117.88$ |
| 3 | DF | Decomposing fragments | $SSA = -16.05 \ln(\rho) + 117.88$ |
| 4 | DF (RG) | Decomposing fragments/rounded grains | $SSA = -16.05 \ln(\rho) + 117.88$ |
| 5 | DF (FC) | Decomposing fragments/faceted crystals | $SSA = -16.05 \ln(\rho) + 117.88$ |
| 6 | PPgp | Graupel | NA |
| 7 | RG | Rounded grains | $SSA = -10.23 \ln(\rho) + 79.56$ |
| 8 | MF (RG) | Rounded grains with limited melting | $SSA = -21.73 \ln(\rho) + 139.97$ |
| 9 | RG (FC) | Faceted rounded grains | $SSA = -10.23 \ln(\rho) + 79.56$ |
| 10 | FC | Faceted crystals | $SSA = -15.07 \ln(\rho) + 96.75$ |
| 11 | FC (DH) | Faceted crystals/depth hoar | $SSA = -15.07 \ln(\rho) + 96.75$ |
| 12 | DH | Depth hoar | $SSA = -6.89 \ln(\rho) + 47.71$ |
| 13 | MF | Melt forms | $SSA = 5.0$ |
| 14 | MF (DH) | Melting depth hoar | $SSA = -21.73 \ln(\rho) + 139.97$ |
| 15 | MF (FC) | Faceted melt forms | $SSA = -21.73 \ln(\rho) + 139.97$ |
| 16 | SH (MF) | Melting surface hoar | $SSA = -21.73 \ln(\rho) + 139.97$ |
| 17 | SH | Surface hoar | $SSA = 34.1$ |
| 18 | IF | Ice forms | $SSA = 2.9$ |

respectively), while these values are nearly same (24.4 and 24.2 cm) in spring months (March and April). The monthly means exhibit the same trends as the monthly medians, showing a large increase from February to March. The monthly mean values of $z_{eu}$ in December, January, February, March, and April are 9.3, 11.4, 15.5, 25.8, and 30.7 cm, respectively. These statistics indicate that the euphotic depths in snow have a clear seasonal variation.

## 3.2. Two key factors in determining the euphotic depth

### *3.2.1. Surface net solar radiation*

The pronounced differences in the euphotic depths between winter and spring may be partly attributed to the seasonal evolution of the surface net solar radiation. Figure 2(c) presents the scatterplot of the relevant surface net solar radiation ($Q_{net}$), and Figure 2(d) shows the corresponding boxplot. Apparently, $z_{eu}$ exhibits a similar seasonal trend with $Q_{net}$. Furthermore, $z_{eu}$ is proportional to $Q_{net}$, as confirmed by a scatter plot of $z_{eu}$ versus $Q_{net}$ in Figure 2(e). The correlation coefficient between $z_{eu}$ and $Q_{net}$ reaches 0.874, which is significant at the 95% confidence level according to the two-tailed Student's $t$ test. This finding implies that surface net solar radiation explains approximately 76.4% of the variation in euphotic depth. In general, with stronger illumination, more energy penetrates through the snowpack, and a deeper euphotic depth is required to attenuate the energy.

However, there are exceptional cases since incident solar radiation is not the only contributor. Some interesting cases [marked as A, B, C, D, and E in Figure 2(e)] are analyzed below as examples. Figure 3(a) shows the vertical profiles of net solar radiation in snow pits: A, B, C, D, and E. The $Q_{net}$ values for A, B, C, D, and E are 24.8, 54.1, 54.4, 51.8, and 152.8 W $m^{-2}$, respectively. According to the above definition of euphotic depth, crossing the gray dash reference line of 1.0 W $m^{-2}$, the values of $z_{eu}$ for A, B, C, D, and E are 6.1, 25.2, 44.6, 48.9, and 49.2 cm, respectively.

To identify other factors that may influence the euphotic depth, these cases were collected in a randomized and controlled manner. B, C, and D exhibit almost the same degree of initial illumination, but their $z_{eu}$ values are quite different. With regard to D and E, the initial $Q_{net}$ of E is nearly three times as much as that of D. However, the $z_{eu}$ of E is nearly equal to that of D. The snow optical properties account for these exceptional cases.

### *3.2.2. Mean extinction coefficient*

Figure 3(b) presents the mean extinction coefficient ($\widetilde{k}$) over increasing depth (Equation (6)). $\widetilde{k}$ decreases with increasing snow depth due to the change in the spectral composition. On the threshold of euphotic depth, $F_{\downarrow}(z_{eu}) = 1.0$ W $m^{-2}$, hence, Equation (6) can be expressed as:

$$\widetilde{k}\Big|_{z_{eu}} = -\left(1/z_{eu}\right) \ln\left(\frac{1}{F_{\downarrow}(0)}\right) = \frac{\ln\left(F_{\downarrow}(0)\right)}{z_{eu}},$$

$$z_{eu} = \frac{\ln\left(F_{\downarrow}(0)\right)}{\widetilde{k}\Big|_{z_{eu}}}. \tag{7}$$

That is to say, there is an inverse proportional relationship between the euphotic depth ($z_{eu}$) and the mean extinction coefficient of the whole euphotic zone ($\widetilde{k}\Big|_{z_{eu}}$). When the light is transmitted to the same depth level, the $\widetilde{k}$ of B (orange line) is greater than those of C (green line) and D (blue line). Hence, under the same level of initial illumination ($F_{\downarrow}(0)$), the $z_{eu}$ of B is less than those of C and D. Similarly, even though the $F_{\downarrow}(0)$ of E is nearly three times as much as that of D, the $\widetilde{k}$ of E is greater than that of D at the same depth level, resulting in nearly the same value of $z_{eu}$. The euphotic depth

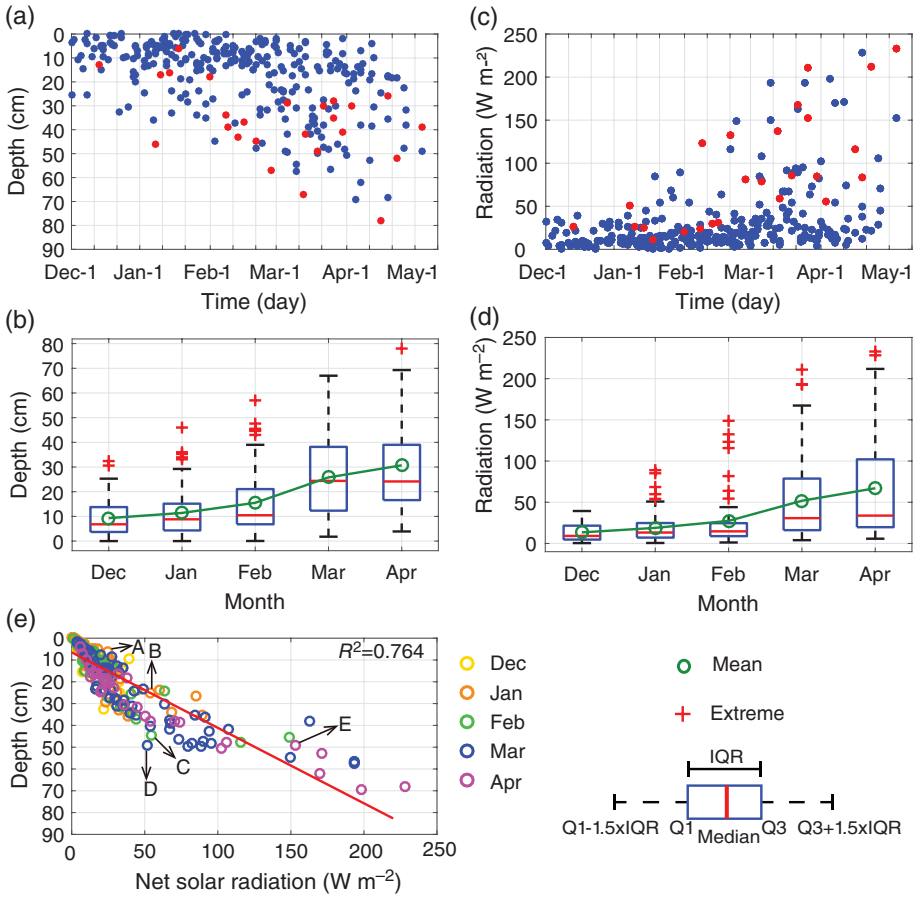


**Figure 2.** (a) Seasonal evolution of the euphotic depth in snow from 302 samples at CDP in 1993–2011 calculated by SNICAR. (c) Seasonal evolution of the surface net solar radiation from 302 samples at CDP in 1993–2011. Red points in (a) and (c) indicate that the solar radiation has already penetrated through to the bottom snow layer completely, and the euphotic depth is marked as its snow depth. (b) and (d) are the boxplot for (a) and (c), respectively. Q1: the first quartiles; Q3: the third quartiles; IQR: interquartile range. (e) Scatter plot of the euphotic depth in snow by SNICAR versus surface net shortwave radiation.

**Table 2.** Detailed values of radiation and optical properties for snow pits A, B, C, D, and E.

| Cases | $Q_{net}$ | $\tau$ (%) | $\widetilde{k}\big\|_{z_{eu}}$ | $z_{eu}$ |
|---|---|---|---|---|
| A | 24.8 | 4.0 | 0.526 | 6.1 |
| B | 54.1 | 1.8 | 0.159 | 25.2 |
| C | 54.4 | 1.8 | 0.090 | 44.6 |
| D | 51.8 | 1.9 | 0.081 | 48.9 |
| E | 152.8 | 0.66 | 0.102 | 49.2 |

Net solar radiation at surface: $Q_{net}$ (W m$^{-2}$); residual percentage: $\tau$ (%); mean extinction coefficient of the whole euphotic zone: $\widetilde{k}\big|_{z_{eu}}$ (cm$^{-1}$); euphotic depth: $z_{eu}$ (cm).

is not only related to the initial solar irradiance but is also attributed to its own snow extinction coefficient. The detailed values are listed in Table 2.

The mean extinction coefficient here is derived from the profile of solar radiation in snow, which follows the exponential law of attenuation. It should be noted that the extinction coefficient is actually a proxy for the effective radius of single particle and the layer mass (snow density) of multiple scattering according to the cause-and-effect reasoning (Wiscombe and Warren, 1980). Both the snow grain effective radius and snow density have a seasonal evolution, as shown in Figure 1, which intensifies the seasonal variability of the euphotic depth from an interior view.

### 3.3. Explanation for the definition of euphotic depth

Figure 3(c) illustrates the residual percentage over snowpack depth, which is an auxiliary explanation for the definition of $z_{eu}$. The residual percentage is the proportion of the remaining downward solar irradiance to the initial solar irradiance beneath the surface, as follows:

$$\tau = \frac{F_{\downarrow}(h)}{F_{\downarrow}(0)}. \tag{8}$$

In aquatic ecology, the euphotic depth is defined as the depth at which photosynthetically available radiation is 1% of value beneath the surface (Lee *et al.,* 2007). For the euphotic depth in snow, it would be nice if we could learn from this definition. However, among the measurements of the beneath surface solar radiation at the CDP station in 1993–2011, the maximum value was 233.0 W m$^{-2}$, and the 25th quantile value was 9.2 W m$^{-2}$, and if following the definition from acoustic ecology, the 1% levels were 2.33 and 0.092 W m$^{-2}$,

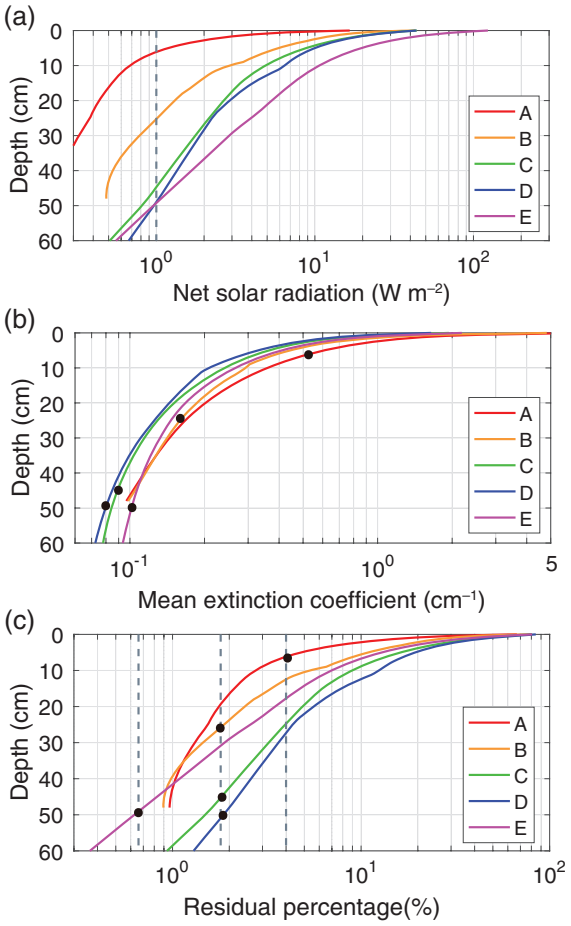


**Figure 3.** Profiles of the samples marked in Figure 2(e), A, B, C, D, and E. (a) Net solar radiation (W m$^{-2}$); (b) Mean extinction coefficient (cm$^{-1}$); Black dot in (b) indicates the cross point of the threshold of euphotic depth and the profile of mean extinction coefficient. (c) Residual percentage (%); Black dot in (c) denotes the cross point of the threshold of euphotic depth and the profile of residual percentage.

respectively, then these values would be inadequate. As they are too lenient for strong radiation cases and too stringent for weak radiation cases. Therefore, we suggest using the definition of euphotic depth in snow as stated in Section 3.1.

On the threshold of euphotic depth, $F_{\downarrow}(z_{eu}) = 1.0$ W m$^{-2}$, and in this way, the remaining percentages for snow pits A, B, C, D, and E are 4.0, 1.8, 1.8, 1.9, and 0.66%, respectively. By cross-referencing these values, the euphotic depth of these pits can also be obtained. Strong initial illumination corresponds to a small residual percentage and vice versa. If the euphotic depth is defined as the depth at which the residual solar radiation is a fixed percentage of the initial irradiation, such as 1.0%, then the results would be strongly biased.

## 4. Conclusions

Solar radiation in the visible bands penetrates through snowpack to a considerable depth, which is called as euphotic depth in this study. The depth is defined here as the depth at which the residual solar radiation began to be <1.0 W m$^{-2}$. The vertical profiles of solar radiation transmitted in the snowpack can be predicted by SNICAR. Most of the variables required by SNICAR are available from regular measurements except for the snow grain effective radius. However, this variable can be estimated from the snow SSA, which can be parameterized using snow type and snow density.

Pronounced differences in the medians, means, and maximums between winter and spring indicated that there was a clear seasonal variation in euphotic depth at CDP. This result may partly owe to the seasonal evolution of net solar radiation. The euphotic depth in snow is proportional to the surface net solar radiation, with the correlation coefficient being as high as 0.874. Exceptional cases were further analyzed and demonstrated that the snow extinction coefficient was the interior contributor influencing the euphotic depth. Stronger illumination and smaller extinction coefficients lead to greater euphotic depths.

Chen *et al.* (2014) inspected the euphotic depths at the same site (CDP, France), using a statistical method (LOcally WEighted Scatterplot Smoothing, LOWESS). The results were 21 and 33 cm in the dry and wet seasons, respectively, which also indicated a seasonal variation in the euphotic depth. Our results are in accordance with theirs but are more detailed and precise. More measurements and investigations are still needed to validate our method.

This study defined the euphotic depth in snowpack and provided a convenient approach to estimating it. This approach may improve our understanding of the differences in the albedo between deep and shallow snowpack in GCMs. In particular, it is important for investigations in regions with relatively shallow snowpack and strong solar radiation, where the euphotic depth is more likely to be great and the albedo is easily affected by the underlying surface. This study left aerosol effects and vegetation canopy out of consideration. As next step, more efforts are needed to understand the relationship between snow depth and snow fraction and the effects of light absorbing aerosols on solar radiation transmission in the snowpack.

## Acknowledgements

We thank two anonymous reviewers for their constructive suggestions and comments, which helped to improve this paper. This study is supported jointly by National Key Basic Research and Development Projects of China (Grant 2014CB953903) and projects from the National Natural Science Foundation of China (Grant 41275003).

## References

Armstrong RL, Brun E. 2008. *Snow and Climate*. Cambridge University Press: Cambridge.

Baker DG, Skaggs RH, Ruschy DL. 1991. Snow depth required to mask the underlying surface. *Journal of Applied Meteorology* **30**: 387–392. https://doi.org/10.1175/1520-0450(1991)030<0387:sdrtmt>2.0.co;2.

Bohren CF, Barkstrom BR. 1974. Theory of optical properties of snow. *Journal of Geophysical Research* **79**: 4527–4535. https://doi.org/10.1029/JC079i030p04527.

Brandt RE, Warren SG. 1993. Solar-heating rates and temperature profiles in Antarctic snow and ice. *Journal of Glaciology* **39**: 99–110.

Brun E, Martin E, Simon V, Gendre C, Coleou C. 1989. An energy and mass model of snow cover suitable for operational avalanche forecasting. *Journal of Glaciology* **35**: 333–342.

Chen AJ, Li WP, Li WJ, Liu X. 2014. An observational study of snow aging and the seasonal variation of snow albedo by using data from Col de Porte, France. *Chinese Science Bulletin* **59**: 4881–4889. https://doi.org/10.1007/s11434-014-0429-9.

Cox PM, Betts RA, Bunton CB, Essery RLH, Rowntree PR, Smith J. 1999. The impact of new land surface physics on the GCM simulation of climate and climate sensitivity. *Climate Dynamics* **15**: 183–203. https://doi.org/10.1007/s003820050276.

Dickinson RE, Kennedy P, Henderson-Sellers A. 1993. *Biosphere-Atmosphere Transfer Scheme (Bats) Version 1e as Coupled to the NCAR Community Climate Model*. National Center for Atmospheric Research, Climate and Global Dynamics Division: Boulder, Colorado, USA.

Domine F, Taillandier AS, Simpson WR. 2007. A parameterization of the specific surface area of seasonal snow for field use and for models of snowpack evolution. *Journal of Geophysical Research* **112**: 13. https://doi.org/10.1029/2006jf000512.

Domine F, Albert M, Huthwelker T, Jacobi H-W, Kokhanovsky A, Lehning M, Picard G, Simpson W. 2008. Snow physics as relevant to snow photochemistry. *Atmospheric Chemistry and Physics* **8**: 171–208.

Douville H, Royer JF, Mahfouf JF. 1995. A new snow parameterization for the Meteo-France Climate Model. 1. Validation in stand-alone experiments. *Climate Dynamics* **12**: 21–35. https://doi.org/10.1007/bf00208760.

Flanner MG, Zender CS. 2005. Snowpack radiative heating: influence on Tibetan Plateau climate. *Geophysical Research Letters* **32**: 5. https://doi.org/10.1029/2004gl022076.

Flanner MG, Zender CS. 2006. Linking snowpack microphysics and albedo evolution. *Journal of Geophysical Research: Atmosphere* **111**: 12. https://doi.org/10.1029/2005jd006834.

Giddings JC, Lachapelle E. 1961. Diffusion theory applied to radiant energy distribution and albedo of snow. *Journal of Geophysical Research* **66**: 181–189. https://doi.org/10.1029/JZ066i001p00181.

Gray DM, Landine PG. 1987. Albedo model for shallow prairie snow covers. *Canadian Journal of Earth Sciences* **24**: 1760–1768. https://doi.org/10.1139/e87-168.

Hadley OL, Kirchstetter TW. 2012. Black-carbon reduction of snow albedo. *Nature Climate Change* **2**: 437–440. https://doi.org/10.1038/nclimate1433.

Hansen J, Russell G, Rind D, Stone P, Lacis A, Lebedeff S, Ruedy R, Travis L. 1983. Efficient three-dimensional global models for climate studies: models I and II. *Monthly Weather Review* **111**: 609–662. https://doi.org/10.1175/1520-0493(1983)111<0609:etdgmf>2.0.co;2.

Järvinen O, Leppäranta M. 2013. Solar radiation transfer in the surface snow layer in Dronning Maud Land, Antarctica. *Polar Science* **7**: 1–17. https://doi.org/10.1016/j.polar.2013.03.002.

Lee Z, Weidemann A, Kindle J, Arnone R, Carder KL, Davis C. 2007. Euphotic zone depth: its derivation and implication to ocean-color remote sensing. *Journal Geophysical Research: Oceans* **112**: 11. https://doi.org/10.1029/2006jc003802.

Meinander O, Kazadzis S, Arola A, Riihelä A, Räisänen P, Kivi R, Kontu A, Kouznetsov R, Sofiev M, Svensson J, Suokanerva H, Aaltonen V, Manninen T, Roujean JL, Hautecoeur O. 2013. Spectral albedo of seasonal snow during intensive melt period at Sodankylä, beyond the Arctic Circle. *Atmospheric Chemistry and Physics* **13**: 3793–3810. https://doi.org/10.5194/acp-13-3793-2013.

Morin S, Lejeune Y, Lesaffre B, Panel JM, Poncet D, David P, Sudul M. 2012. An 18-yr long (1993–2011) snow and meteorological dataset from a mid-altitude mountain site (Col de Porte, France, 1325m alt.) for driving and evaluating snowpack models. *Earth System Science Data* **4**: 13–21. https://doi.org/10.5194/essd-4-13-2012.

Morin S, Domine F, Dufour A, Lejeune Y, Lesaffre B, Willemet JM, Carmagnola CM, Jacobi HW. 2013. Measurements and modeling of the vertical profile of specific surface area of an alpine snowpack. *Advances in Water Resources* **55**: 111–120. https://doi.org/10.1016/j.advwatres.2012.01.010.

Oleson KW, Lawrence DM, Gordon B, Flanner MG, Kluzek E, Peter J, Levis S, Swenson SC, Thornton E, Feddema J, Heald CL, Lamarque J-f, Niu G, Qian T, Running S, Sakaguchi K, Yang L, Zeng X, Zeng X, Decker M. 2010. *Technical Description of version 4.0 of the Community Land Model (CLM)*. National Center for Atmospheric Research: Boulder, CO.

O'Neill A, Gray DM. 1972. Solar radiation penetration through snow. The Role of Snow and Ice in Hydrology, Proceedings of the Banff Symposium, International Association of Hydrology Science 107, 227–240.

Perovich DK. 2007. Light reflection and transmission by a temperate snow cover. *Journal of Glaciology* **53**: 201–210. https://doi.org/10.3189/172756507782202919.

Toon OB, McKay CP, Ackerman TP, Santhanam K. 1989. Rapid calculation of radiative heating rates and photodissociation rates in inhomogeneous multiple-scattering atmospheres. *Journal Geophysical Research: Atmosphere.* **94**: 16287–16301. https://doi.org/10.1029/JD094iD13p16287.

Verseghy DL. 1991. Class-A Canadian land surface scheme for GCMS. 1. Soil model. *International Journal of Climatology* **11**: 111–133.

Wiscombe WJ, Warren SG. 1980. A model for the spectral albedo of snow. I: pure snow. *Journal of the Atmospheric Sciences* **37**: 2712–2733. https://doi.org/10.1175/1520-0469(1980)037<2712:AMFTSA>2.0.CO;2.

Zhong EF, Li Q, Sun SF, Chen W, Chen SF, Nath D. 2017. Improvement of a snow albedo parameterization in the Snow–Atmosphere–Soil Transfer model: evaluation of impacts of aerosol on seasonal snow cover. *Advances in Atmospheric Sciences* **34**: 1333–1345. https://doi.org/10.1007/s00376-017-7019-0.